Novel fabrication method of diverse one-dimensional Pt/ZnO hybrid nanostructures and its sensor application

2011 Nanotechnology 22 035601

(http://iopscience.iop.org/0957-4484/22/3/035601)

Nanotechnology **22** (2011) 035601 (8pp) doi:10.1088/0957-4484/22/3/035601

Novel fabrication method of diverse one-dimensional Pt/ZnO hybrid nanostructures and its sensor application

Mi Ae Lim[1,2,4], **Young Wook Lee**[2,3,4], **Sang Woo Han**[2,3,5] **and Inkyu Park**[1,2,5]

[1] Department of Mechanical Engineering, Korea Advanced Institute of Science and Technology, Daejeon, 305-701, Republic of Korea
[2] KAIST Institute for the NanoCentury, Korea Advanced Institute of Science and Technology, Daejeon, 305-701, Republic of Korea
[3] Department of Chemistry, Korea Advanced Institute of Science and Technology, Daejeon, 305-701, Republic of Korea

E-mail: sangwoohan@kaist.ac.kr and inkyu@kaist.ac.kr

Received 24 September 2010
Published 9 December 2010
Online at stacks.iop.org/Nano/22/035601

Abstract

A novel low-temperature, solution-phase method for the facile fabrication of a variety of one-dimensional (1D) metal/metal oxide hybrid nanostructures has been developed. This method is based on the wet chemical synthesis of metal oxide nanowires, followed by the surface coating of metal nanoparticles on metal oxide nanowire templates via reduction of metal ions along with controlled etching of metal oxide nanowires at the core, all in a low-temperature liquid environment. As a proof-of-concept, we applied this method to the fabrication of various 1D Pt/ZnO hybrid nanostructures including Pt nanoparticle-coated ZnO nanowires/nanotubes and Pt nanotubes on silicon and polymer substrates. The diverse morphology tuning is attributed to the control of pH in the solution with different metal precursor concentrations and amounts of reducing agent. The change of morphology, crystalline structure, and composition of various 1D Pt/ZnO hybrid nanostructures was observed by SEM, TEM (HRTEM), XRD and ICP-AES, respectively. Further, we have demonstrated a highly sensitive strain sensor (gauge factor = 15) with a Pt nanotube film fabricated by the developed method on a flexible polymer substrate.

S Online supplementary data available from stacks.iop.org/Nano/22/035601/mmedia

(Some figures in this article are in color only in the electronic version)

1. Introduction

One-dimensional (1D) nanostructures such as nanowires, nanotubes and nanobelts have received considerable attention owing to their various potential applications deriving from their unique physical and chemical properties. Therefore, a number of techniques have been developed for the fabrication of 1D nanostructured materials [1–3]. Among them, 1D Pt and Pd nanostructures have been extensively studied for use as catalysts for many chemical reactions, electrode materials in fuel cells, and sensing materials in gas sensors [4].

The preparation of 1D Pt and Pd nanostructures is usually based on template-assisted synthesis, including the use of hard templates [5, 6] or soft templates [7–9]. Recently, the galvanic displacement method has proven to be a remarkably simple and versatile route for preparing nanostructures with controllable hollow interiors and porous surfaces [10]. Pt and Pt–Pd (platinum–palladium alloy) nanotubes were synthesized from the galvanic displacement reaction using tellurium or silver nanowires as templates [11–14], and their electrocatalytic activities were investigated for methanol oxidation reaction of DMFC (direct methanol fuel cells) [13] and oxygen reduction reaction of PEMFC (proton exchange membrane fuel cells) [14], respectively.

[4] These authors contributed equally to this work.
[5] Authors to whom any correspondence should be addressed.

As another important nanomaterial, 1D nanostructures of ZnO with a wide band gap (3.37 eV) and a large excitation binding energy (∼60 meV) have attracted much attention due to their significant applications in optics, optoelectronics, sensors, and actuators [15–19]. Single crystalline ZnO nanowires are most commonly synthesized by template-based processing [20], solution methods [21–24] and gas-phase approaches such as metal–organic chemical vapor deposition [25, 26], chemical vapor transport [27, 28], and pulsed laser deposition [29]. Among them, the solution-based reaction takes advantage of low-temperature, large scale and an economical synthesis method. The preparation of ZnO nanowires from an aqueous solution of zinc nitrate and hexamethylenetetramine (HMTA) via a hydrothermal process was developed by Vayssieres *et al* [21]. Afterward, well-aligned ZnO nanowire arrays were produced using substrates coated with ZnO seeds by Yang *et al* [22–24]. Solution-grown ZnO nanowire arrays on the substrate were used as an efficient photoanode in dye sensitized solar cells (DSSC) [23, 24]. On the other hand, studies on ZnO nanowires coated with noble metal nanoparticles (Pt, Pd and Au) were carried out to enhance the sensitivities of ZnO nanowire-based gas/vapor sensors [30–33]. The surface modification of ZnO nanowires with metal nanoparticles enhances the catalytic reaction with analyte molecules and results in improved sensitivity of the ZnO nanowire-based sensors.

However, so far, the studies on the metal–ZnO hybrid nanostructures have been mainly focused on the decoration of ZnO nanowires with metal nanoparticles only. In this work, a simple solution process to fabricate various 1D Pt/ZnO hybrid nanostructures with tunable shapes on the substrate has been demonstrated using the reaction between ZnO nanowires grown on the substrate and aqueous solution of Pt salt. 1D Pt/ZnO nanostructures of various morphologies including Pt nanoparticles (NPs) coated ZnO nanowires, Pt/ZnO hybrid nanotubes, and Pt nanotubes were prepared by the control of synthesis conditions such as pH, Pt salt concentration, and amount of sodium citrate in the solution. Due to the low-temperature and mild chemical conditions, this process is also compatible with flexible polymer substrates. For potential flexible sensor applications, a film of Pt nanotubes was fabricated on a polyimide substrate by using the developed method. The strain sensitivity of electrical resistance of Pt nanotube film was characterized by applying bending deformation for the first time. The fabricated Pt nanotube film exhibited a potential applicability as a strain sensor with high strain sensitivity (gauge factor = 15).

2. Experimental procedures

2.1. Chemicals

Zinc acetate dehydrate ($Zn(CH_3COO)_2{\cdot}2H_2O$, Aldrich, 99.999%), zinc nitrate hexahydrate ($Zn(NO_3)_2{\cdot}6H_2O$, Aldrich, 98%), hexamethylenetetramine (HMTA, Aldrich, 99+%), polyethylenimine (PEI, Aldrich, molecular weight: 800), sodium hydroxide (NaOH, Junsei, 97%), nitric acid (HNO_3, Junsei, 60–61%), potassium tetrachloroplatinate (II) (K_2PtCl_4, Aldrich, 98%) and sodium citrate dihydrate (Aldrich, 99%) were used as received without further purification. Methanol, acetone, IPA (isopropyl alcohol), and ethanol were purchased from Daejung Chemicals & Metals Co., Ltd.

2.2. Preparation of ZnO nanowire arrays on substrates

Vertical ZnO nanowire arrays were prepared on Si and polyimide substrates, similar to the method by Yang *et al* [22–24]. Prior to the growth of ZnO nanowire arrays, the Si and polyimide substrates were cleaned by ultrasonication in acetone/IPA/ethanol/de-ionized water, and methanol solution, and subsequently dried by nitrogen gas. In the first step, to form the film of ZnO nanocrystal seeds, ZnO nanoparticle solution was prepared based on the literature [34]. The substrates were wetted with a droplet of ZnO nanoparticle dispersion (in methanol), rinsed with ethanol, and then blow-dried with nitrogen gas. This step was repeated several times for a complete coverage of seeds and the substrate was annealed at 150 °C for 10 min. ZnO nanowire arrays were then grown hydrothermally by immersing the seeded substrate in aqueous solutions containing zinc nitrate (25 mM), HMTA (25 mM), and PEI (6 mM) at 95 °C for 2.5 h. The substrate was then removed from solution, washed with de-ionized water, and blow-dried.

2.3. Morphology control of 1D Pt/ZnO nanostructures

For the preparation of 1D Pt/ZnO hybrid nanostructure, Si and polyimide substrates with ZnO nanowire arrays were fixed on the polytetrafluoroethylene (PTFE) holder and immersed in a container filled with 2–3 ml of the aqueous solution of K_2PtCl_4 (1–5 mM) with sodium citrate solution (30 mM). In addition, the pH of the mixture solution was adjusted by adding HNO_3 (0.1 M) or NaOH (0.01 and 0.1 M) solution and the amount of sodium citrate solution was varied (10–100 μl) in order to control the morphology of the Pt/ZnO nanostructures. The container was closed and maintained at 90 °C for 1 h in a conventional convection oven. After the reaction, the samples were taken out and washed several times with triply distilled water and ethanol.

2.4. Characterizations

Scanning electron microscopy (SEM) images of the samples were taken with a field emission scanning electron microscope (FESEM, Phillips Model XL30 FEG). Transmission electron microscopy (TEM) images were obtained with a Phillips Model Technai F20 transmission electron microscope operating at 200 kV after placing a drop of the aqueous dispersion of Pt/ZnO nanostructures, which was obtained by sonication treatment of 1D Pt/ZnO nanostructures on Si substrate, onto the carbon-coated copper grids (200 mesh). High resolution TEM (HRTEM) and high-angle annular dark-field scanning TEM (HAADF-STEM) characterization were performed with an FEI Technai G2 F30 Super-Twin transmission electron microscope operating at 300 kV. The effective electron probe size and dwell time used in HAADF-STEM-energy-dispersive x-ray spectroscopy (EDS) mapping experiments were 1.5 nm and

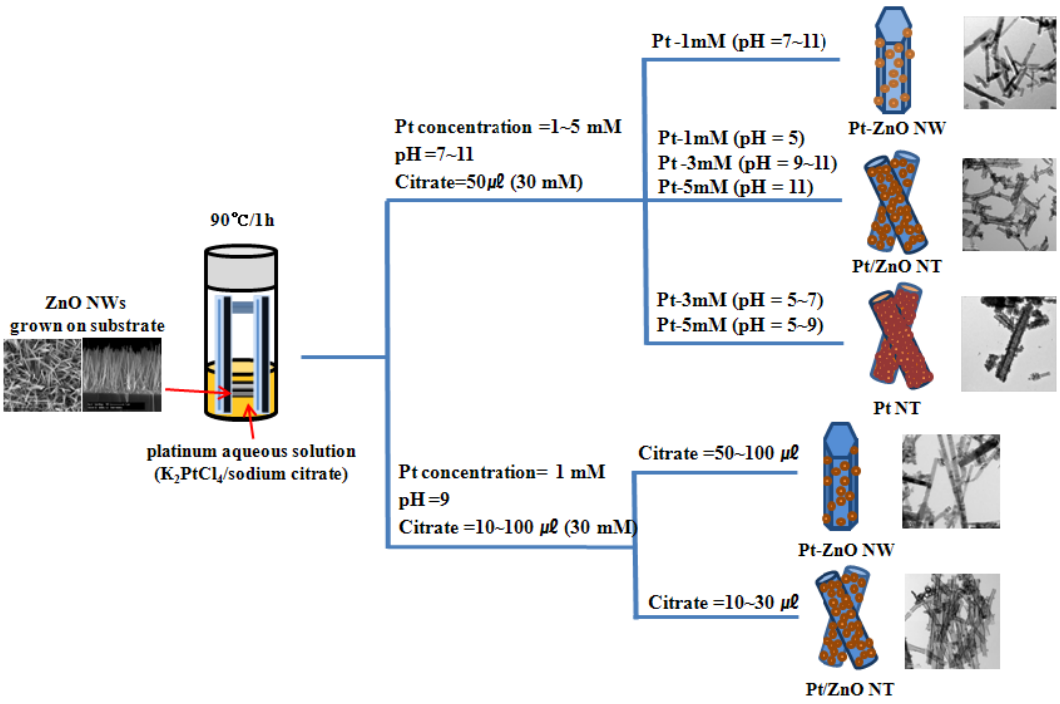

Figure 1. Schematic illustrations showing the formation processes of various 1D Pt/ZnO hybrid nanostructures.

200 ms/pixel, respectively. The compositions of Pt and Zn in the Pt/ZnO nanostructure were quantified by an inductively coupled plasma atomic emission spectrometer (ICP-AES, OPTIMA 330DV). X-ray diffraction (XRD) patterns were obtained with a Bruker AXS D8 DISCOVER diffractometer using Cu Kα (0.1542 nm) radiation.

2.5. Measurement of electrical properties and strain sensitivity

For current–voltage (I–V) measurement, copper wire electrodes were attached with silver paste to the opposite sides of the Pt nanotube film prepared on the polyimide substrate. The total length of sample was 2.6 cm while the two electrodes were attached at 0.5 cm from each edge of the sample. The width and thickness of the polyimide substrate were approximately 0.5 cm and 75 μm respectively. I–V curves were obtained by a linear sweep voltammetry method using a CHI 600D electrochemical analyzer. To investigate strain-induced resistance change of the Pt nanotube film, the polyimide substrate coated with Pt nanotubes was mounted on the carrier substrate (polycarbonate film, length = 5 cm, width = 2 cm, thickness = 0.2 mm). Bending of the film was performed by decreasing the distance between two one-axis linear stages to which the two ends of the carrier substrate were attached. The resulting strain (ε) from the bending can be estimated using the following equation:

$$\varepsilon = (D/T + 1)^{-1}.$$

Here D is the diameter of the bending film and T is the thickness of the substrate. The average resistance of the Pt nanotube film under varying bending deformation was calculated from I–V sweep measurements (repeated ten times). The experimental setup for the strain sensor test is summarized in figure S1 (available at stacks.iop.org/Nano/22/035601/mmedia).

3. Results and discussion

The formation process of tunable 1D Pt/ZnO hybrid nanostructures is illustrated in figure 1. 1D Pt/ZnO hybrid nanostructures with a variety of morphologies such as Pt NPs-coated ZnO nanowires, Pt/ZnO hybrid nanotubes, and Pt nanotubes were prepared by the low-temperature reaction between ZnO nanowires grown on Si substrate and aqueous solutions of Pt precursor. The structure tuning of the hybrid nanostructures is achieved by control of the experimental parameters such as pH, Pt salt concentration, and amount of sodium citrate in the aqueous solution of the Pt precursor. The configuration of hybrid nanostructures is changed from Pt NP-coated ZnO nanowires to Pt/ZnO hybrid nanotubes, and finally to Pt nanotubes as the initial pH is decreased and also as the concentration of Pt salt is increased. In addition, the relative composition of Pt to Zn is increased when the amount of citrate, which acts both as a reducing agent and a stabilizer, is decreased. Various morphologies of 1D Pt/ZnO hybrid nanostructures were investigated by SEM and TEM measurements as shown in figures 2–4.

Figure 2 shows SEM ((A)–(E)), TEM ((F)–(J)), and HRTEM ((K)–(O)) images of 1D Pt/ZnO nanostructures prepared from ZnO nanowires and the aqueous solution of Pt precursor with different Pt salt concentrations (1–5 mM) and pH (5–11). The aqueous solution of Pt precursor was prepared by mixing K_2PtCl_4, triply distilled water, and sodium

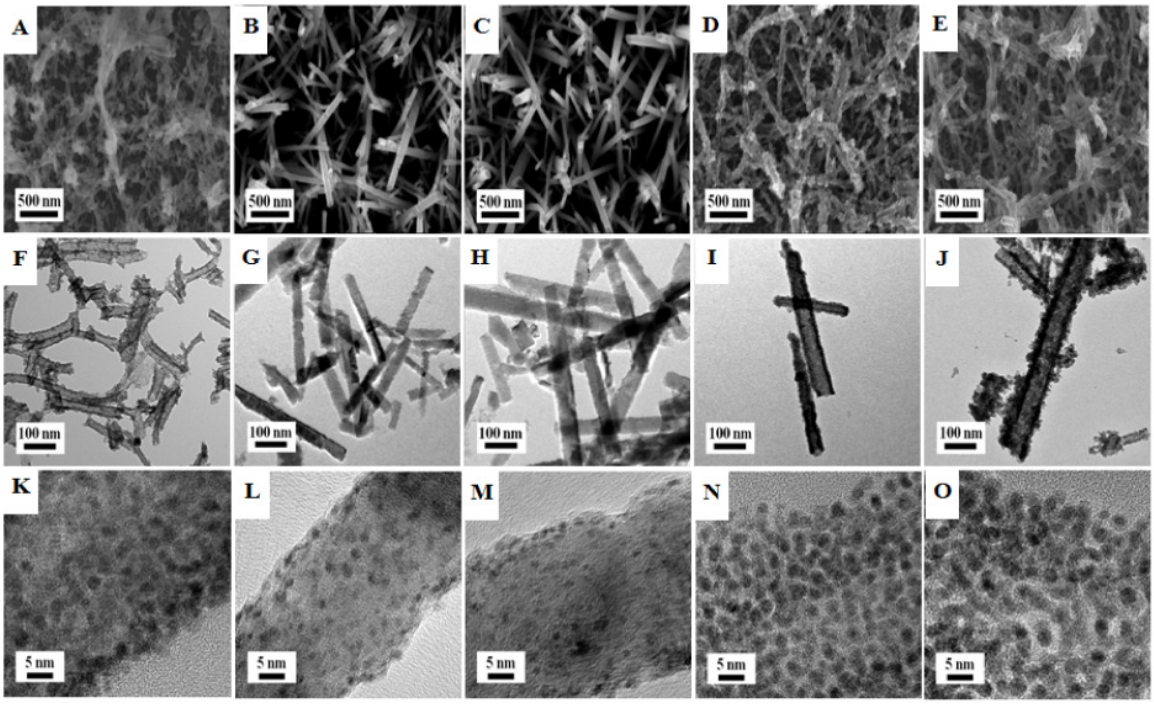

Figure 2. SEM ((A)–(E)), TEM ((F)–(J)) and HRTEM ((K)–(O)) images of 1D Pt/ZnO hybrid nanostructures prepared from ZnO nanowires and the aqueous solution of Pt precursor with different Pt salt concentrations (1–5 mM) and pH values (5–11). ((A), (F), (K)) $[PtCl_4^{2-}] = 1$ mM, pH 5; ((B), (G), (L)) $[PtCl_4^{2-}] = 1$ mM, pH 7; ((C), (H), (M)) $[PtCl_4^{2-}] = 1$ mM, pH 11; ((D), (I), (N)) $[PtCl_4^{2-}] = 3$ mM, pH 7; ((E), (J), (O)) $[PtCl_4^{2-}] = 5$ mM, pH 7.

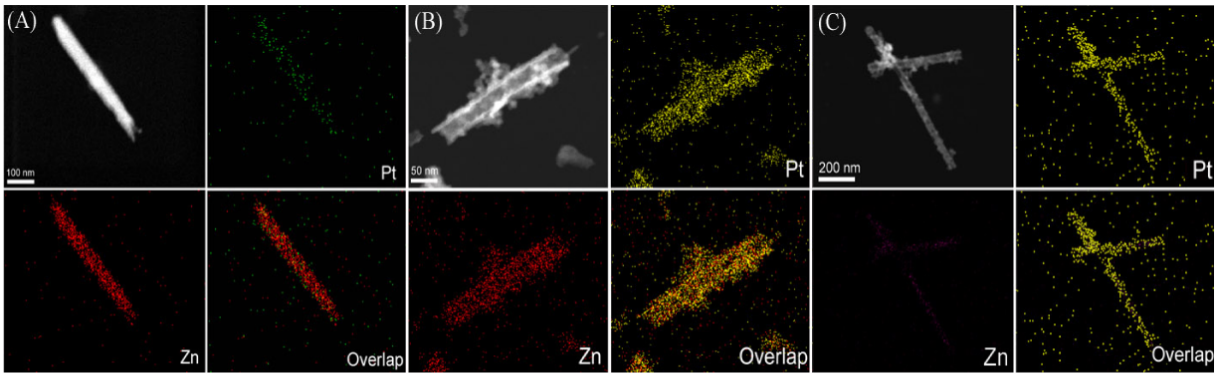

Figure 3. HAADF-STEM-EDS mapping images of 1D Pt/ZnO hybrid nanostructures, which were selected from the three sections: (A) $[PtCl_4^{2-}] = 1$ mM, pH 9; (B) $[PtCl_4^{2-}] = 3$ mM, pH 11; (C) $[PtCl_4^{2-}] = 5$ mM, pH 7.

citrate solution (30 mM). The amount of citrate added into the solution was fixed at 50 μl and the pH of the mixture solution was adjusted by adding HNO_3 (0.1 M) or NaOH (0.01 and 0.1 M) solution. The SEM and TEM images in figure S2 (available at stacks.iop.org/Nano/22/035601/mmedia) show that the ZnO nanowires grown by the hydrothermal synthesis method have diameters and lengths in the ranges 35–80 nm and 1–2 μm, respectively. The clear lattice fringes observed in the HRTEM image in figure S2 (available at stacks.iop.org/Nano/22/035601/mmedia) indicate that the nanowires have a single crystalline structure. The morphology of hybrid nanostructures using ZnO nanowires as template was transformed from ZnO nanowires (pH = 7 and 11) to nanotubes (pH = 5) with their surface coated by Pt NPs according to the change of pH in the aqueous solution of Pt precursor with 1 mM Pt salt concentration. It was confirmed from the HRTEM images that single crystalline Pt NPs of size about 2–3 nm were formed sparsely along the surfaces of the ZnO nanowires and nanotubes due to the reduction of the metal precursors ($PtCl_4^{2-}$). On the contrary, the nanostructures prepared from high concentration Pt precursor solutions ($[PtCl_4^{2-}]$ = 3 and 5 mM, pH = 7) consist of ZnO nanotubes that are densely covered with Pt NPs with diameters of 3–4 nm. The agglomeration of nanoparticles on the surfaces of nanotubes was observed. Other nanostructures prepared from 3 and 5 mM Pt salt solutions with different pH (5 and 11) also have similar shapes.

In order to better understand the formation process of tunable 1D Pt/ZnO hybrid nanostructures, the change of pH (initially at pH = 5–11) of aqueous solution of Pt precursor

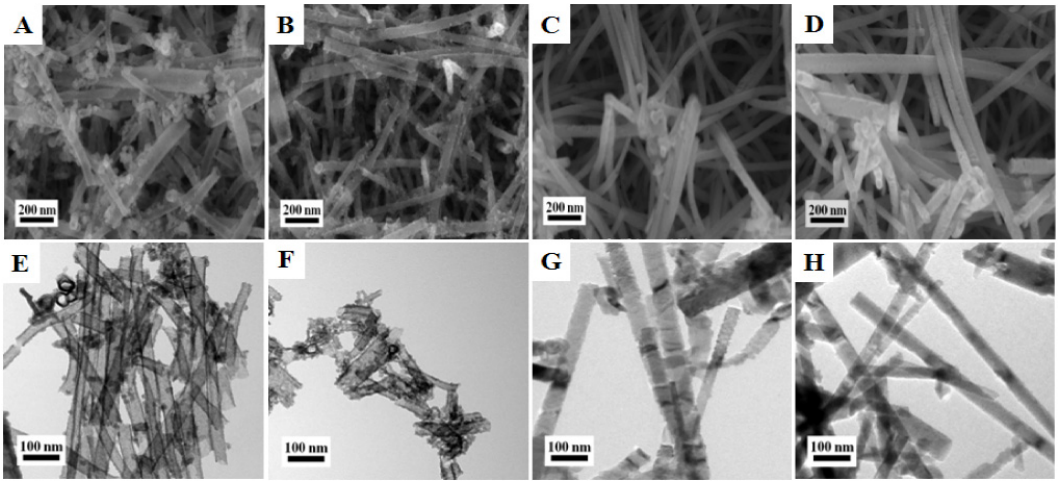

Figure 4. SEM ((A)–(D)) and TEM ((E)–(H)) images of 1D Pt/ZnO hybrid nanostructures prepared from 1 mM Pt precursor solution with different amounts of citrate (initial pH = 9): ((A), (E)) 10 μl, ((B), (F)) 30 μl, ((C), (G)) 50 μl, ((D), (H)) 100 μl.

Table 1. Chemical analysis of ZnO/Pt hybrid nanostructure prepared at different Pt salt concentrations and initial pH: change of pH in the Pt precursor solution and final molar percentages of Zn and Pt in 1D Pt/ZnO hybrid nanostructures after the reaction at 90 °C for 1 h. White box, section I: Pt NP-coated ZnO nanowire. Gray box, Section II: Pt/ZnO hybrid nanotube. Dark gray box, section III: Pt nanotube.

1 mM (Pt con.)				3 mM				5 mM			
pH (before/after)		Zn (mol%)	Pt (mol%)	pH (before/after)		Zn (mol%)	Pt (mol%)	pH (before/after)		Zn (mol%)	Pt (mol%)
5	4.3	10	90	5	3.9	1	99	5	3.8	1	99
7	5.2	85	15	7	4.0	1	99	7	4.0	1	99
9	6.0	94	6	9	4.5	30	70	9	4.0	1	99
11	7.1	94	6	11	4.8	60	40	11	4.2	11	89

with different Pt salt concentrations was measured throughout the reaction with ZnO nanowires. The composition analysis of Pt and Zn in Pt/ZnO hybrid nanostructure was carried out by using ICP-AES. As shown in table 1, the pH value of aqueous solution of Pt precursor initially at pH = 5–11 decreased after the reaction. In particular, the reduction of pH value was noticeable as the Pt salt concentration in the solution was increased. The decrease of pH value in the solutions is attributed to the reduction of metal ions in the aqueous solution of Pt precursor. Figure S4 (available at stacks.iop.org/Nano/22/035601/mmedia) shows the temporal change of pH in aqueous solution of Pt precursor with and without ZnO nanowires during the reaction at 90 °C for 1 h. Here, the initial Pt salt concentrations were 1, 3, and 5 mM and the initial pH value was fixed to 7. The pH of the aqueous solution of Pt precursor without ZnO nanowires was decreased rapidly with increasing reaction time. This can be the result of the consumption of OH^- ions in the reaction mixture during the reduction of $PtCl_4^{2-}$ by citrate [35] and the reaction mixture turns into the acidic condition as a consequence. Therefore, as shown in figure S4 (available at stacks.iop.org/Nano/22/035601/mmedia), the final acidity is stronger for solution with higher Pt salt concentration ($[PtCl_4^{2-}] = 1$ mM $\rightarrow$ pH = 4.6, $[PtCl_4^{2-}] = 3$ mM $\rightarrow$ pH = 3.8, $[PtCl_4^{2-}] = 5$ mM $\rightarrow$ pH = 3.9). Generally, it has been known that ZnO, as an amphoteric oxide, can react with both H^+ and OH^- ions in acidic and alkaline solutions, respectively, and the products are soluble salt [36, 37]. ZnO is dissolved by the reaction with H^+ ions in acidic aqueous solution of Pt precursor according to the following reaction:

$$ZnO + 2H^+ \rightarrow Zn^{2+} + H_2O \qquad \text{(in acid solution)}.$$

Therefore, the pH value of aqueous solution of Pt precursor with ZnO nanowires is slightly higher than that without ZnO nanowires due to the neutralization effect of ZnO nanowires, which act as a weak base. However, the amount of ZnO is still not sufficient to significantly suppress the decrease of pH caused by the reduction of metal precursors in aqueous solution of Pt precursor as observed in figure S4 (available at stacks.iop.org/Nano/22/035601/mmedia). In addition, the molar percentage of Zn in Pt/ZnO hybrid nanostructures was diminished with lower initial pH and higher Pt salt concentration of precursor solution. This is due to faster dissolution of ZnO by H^+ at lower pH that is further strengthened by more active reduction of $PtCl_4^{2-}$ at higher Pt concentration of the solution. 1D ZnO nanostructures of wurtzite crystal structure have a hexagonal unit cell, which is composed of six nonpolar $\{10\bar{1}0\}$ prismatic faces and two polar planes, i.e., the $(000\bar{1})$ and (0001) planes. Recently, the formation of ZnO nanotubes by selective etching of ZnO nanorods in the (0001) planes due to remarkably different etching rates between the nonpolar and polar planes in acidic or alkaline solutions has been reported by She *et al* [37]. Therefore, it can be speculated that 1D Pt/ZnO hybrid nanostructures are transformed from Pt NP-coated ZnO

nanowires to Pt/ZnO nanotubes due to the selective etching of ZnO nanowires along the axial direction in the acidic Pt precursor solution.

Especially, it is observed that the Pt/ZnO nanotubes prepared from 3 and 5 mM aqueous solution of Pt precursor with low initial pH of 5–7 contain much lower molar percentage ($\leqslant$1 mol%) of Zn than those obtained from other conditions. Table 1 presents three different sections of Pt/ZnO hybrid nanostructure configurations according to the relative quantity of Zn (large, intermediate, small) in the fabricated Pt/ZnO hybrid nanostructures (section I: 85 mol% $\leqslant$ Zn $\leqslant$ 94 mol%, section II: 10 mol% $\leqslant$ Zn $\leqslant$ 60 mol%, and section III: Zn $\leqslant$ 1 mol%). The nanostructures representing each section were selected (section I: $[PtCl_4^{2-}] = 1$ mM and pH = 9; section II: $[PtCl_4^{2-}] = 3$ mM and pH = 11; section III: $[PtCl_4^{2-}] = 5$ mM and pH = 7) and characterized by HAADF-STEM and XRD measurement. Figure 3 shows HAADF-STEM-EDS mapping images of 1D Pt/ZnO hybrid nanostructures, selected from the three sections of table 1. The intensity of Pt element is much weaker than that of Zn element for (A) $[PtCl_4^{2-}] = 1$ mM and pH = 9, while the opposite phenomenon is observed for (C) $[PtCl_4^{2-}] = 5$ mM and pH = 7. From these elemental mapping results, we can conclude that Pt NP-coated ZnO nanowires, Pt/ZnO hybrid nanotubes, and Pt nanotubes were synthesized in sections I, II, and III, respectively. Figure S5 (available at stacks.iop.org/Nano/22/035601/mmedia) shows the XRD pattern of fabricated Pt nanotubes (in section III) in comparison with that of pure ZnO nanowires. Here, the diffraction peaks of Pt can be observed clearly, and can be indexed to the face-centered cubic (fcc) phase. Sharp diffraction peaks of Pt and no traces of ZnO peaks indicate that the Pt NPs were well crystallized along the ZnO nanowire templates while etching away ZnO nanowires.

The amount of sodium citrate affects the morphologies and compositions of the Pt/ZnO hybrid nanostructures as shown in figure 4 and table 2. Figure 4 shows SEM ((A)–(D)) and TEM ((E)–(H)) images of 1D Pt/ZnO nanostructures prepared from ZnO nanowires immersed in 1 mM aqueous solution of Pt precursor at pH = 9 mixed with different amounts of sodium citrate solution (30 mM). The hybrid nanostructures synthesized from the aqueous solution of Pt precursor with citrate of 10 and 30 μl take the shape of Pt/ZnO hybrid nanotubes, while those prepared in the solution with citrate of 50 and 100 μl have Pt NP-coated ZnO nanowire. This morphology change is attributed to the reduction of pH value in the aqueous solution of Pt precursor with smaller amount of sodium citrate. Since citrate is the conjugate base of citric acid (weak acid), decreasing the amount of citrate should induce the decrease of pH, which promotes the directional etching of ZnO and formation of ZnO nanotubes. Table 2 shows the effect of citrate amount on the change of pH of the aqueous solution of Pt precursor and molar percentages of Zn and Pt after the synthesis of Pt/ZnO hybrid nanostructures. The final value of pH in the aqueous solution of Pt precursor after the reaction was reduced from 6.8 to 5.5 as the amount of citrate was decreased from 100 to 10 μl. Accordingly, the relative content of Zn was decreased with the formation of Pt/ZnO nanotubes rather than Pt NP-coated ZnO nanowires by accelerated etching of ZnO at lower pH condition.

Table 2. pH in the Pt precursor solution with different citrate amounts, measured before and after the reaction with ZnO nanowires, and content (mol%) of Zn and Pt in the hybrid nanostructures estimated from ICP-AES analysis.

Citrate content (μl)	pH (before/after)		Zn (mol%)	Pt (mol%)
10	9.0	5.5	46	54
30	9.0	5.8	80	20
50	9.0	6.3	95	5
100	9.0	6.8	95	5

In summary, the developed simple solution process based on the reaction between ZnO nanowires and aqueous solution of Pt precursor allows facile and direct integration of a variety of 1D Pt/ZnO hybrid nanostructures with good tunability in morphologies and compositions. Furthermore, this process is also compatible with flexible polymer substrates due to the low-temperature and mild chemical conditions. Pt nanotube film was prepared using the aforementioned experimental conditions with hydrothermally grown ZnO nanowires on the polyimide substrate for its application as a flexible strain sensor. The Pt salt concentration and initial pH in the aqueous solution of Pt precursor used for reaction were 3 mM and pH = 7, respectively. The strain sensitivity of electrical resistance of the Pt nanotube film was characterized by bending the polyimide substrate coated with Pt nanotubes. Figure 5(a) shows typical I–V characteristics of the Pt nanotube film measured in room temperature, atmospheric conditions under varying strains (ε). The I–V curves present the average values obtained from ten voltage sweep measurements. The measurements reveal Ohmic behavior of the Pt nanotube film over the whole strain range. Also, the conductivity of the Pt nanotube film was reduced as the strain was increased. The relative change in the electrical resistance ($\Delta R/R_0$) of the Pt nanotube film in response to the change of the strain (ε) applied on the film is depicted in figure 5(b). Although the resistance–strain curve exhibits a large standard deviation at $\varepsilon = 0.002$ in the bending cycle, the resistance generally shows approximately linear dependence on the strain applied to the Pt nanotube film for $\varepsilon = 0$–0.004. The average gauge factor defined as the ratio of normalized change in electrical resistance to the strain ($(\Delta R/R_0)/\varepsilon$) was calculated to be $G_S = \sim$15 in Pt nanotube film, which greatly exceeds the typical gauge factor ($G_S \sim 2$) of conventional strain gauges based on metal foils. In order to investigate the reversibility of the strain sensor based on Pt nanotube film, the change in resistance was measured while relaxing the film in the opposite direction by unbending the polyimide substrate. The electrical resistance returned to the original value initially measured before the bending test. This indicates that the structural changes and strain gauge performance of Pt nanotube film are reversible for repeated usage as a highly sensitive strain sensor.

Generally, the charge-transport process in metal NP films takes places via the electron tunneling process between NPs and the tunnel resistance of films depends exponentially on the average interparticle distances working as tunnel barriers [38]. The strain sensitivity of ligand-capped Au NP films on flexible polymer substrate has been previously

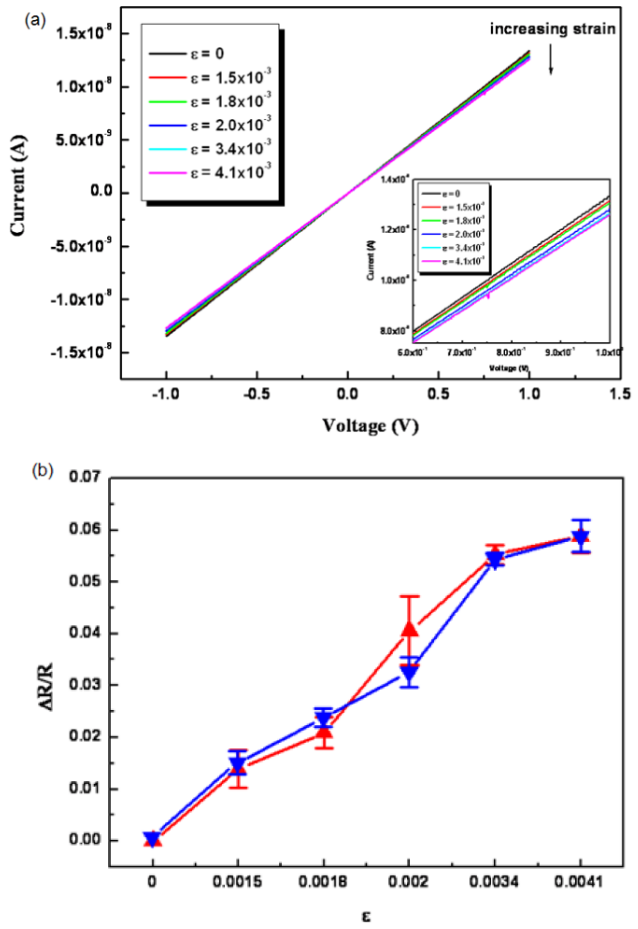

Figure 5. (a) I–V characteristics of Pt nanotube film at different strains. (b) Normalized change in the resistance ($\Delta R/R_0$) of Pt nanotube film as a function of the strain (ε). The red triangles are data points measured in the direction of increasing strain. The data points shown as blue triangles were measured in the opposite direction. (Color in online version).

investigated [39, 40]. The electrical resistance of Au NP films increased in accordance with the change of the strain applied on the films, which is explained by the increase of tunnel barrier width due to the increase of interparticle distance. The strain sensitivity of Pt nanotube films can also be explained by a similar mechanism. As observed in figures 2(D), (I) and (N), Pt nanotube film consists of numerous Pt nanoparticles that are closely packed with small interparticle distances. Under mechanical strain, the interparticle distances may slightly increase, causing the increase of tunnel resistance. This results in the increase of overall electrical resistance of Pt nanotube film. Further, the Pt nanotube film looks like a porous sponge-like structure formed by myriads of electrical connections between Pt nanotubes, many of which may have low physical bond strength. As higher strain is applied, more disconnection between Pt nanotubes will occur, thereby hampering the electron transport through the film. Therefore, it can be summarized that the high strain sensitivity of Pt nanotube film may originate from (1) change of tunneling current between neighboring Pt NPs and (2) change of electrical connection number between adjacent Pt nanotubes. The Pt nanotube film fabricated in this work shows comparable gauge factors ($G_S = \sim 15$) to those of the strain gauges based on Au NP thin films in the literature (G_S = 50–100 by Hermann *et al* [38] and G_S = 10–20 by Vossmeyer *et al* [39]).

4. Conclusion

1D Pt/ZnO hybrid nanostructures with tunable morphologies and compositions were prepared on substrate via simple solution-phase synthesis by the reaction between hydrothermally grown ZnO nanowires and aqueous solution of Pt precursor under moderate temperature and mild chemical conditions. The structural tuning of 1D Pt/ZnO hybrid nanostructures including Pt NP-coated ZnO nanowires, Pt/ZnO hybrid nanotubes, and Pt nanotubes was achieved by varying synthesis parameters such as pH, Pt salt concentration, and citrate amount in the aqueous solution of Pt precursor. This morphology change is attributed to the etching effect of ZnO nanowires in the acidic condition that is enhanced by the decrease of pH in the solution via the reduction of metal precursors ($PtCl_4^{2-}$) into Pt NPs. Pt nanotube film was prepared on flexible polyimide film by this novel method and its strain sensitivity was characterized under a bending experiment of the polyimide substrate. The normalized change in electrical resistance of Pt nanotube film increased in linear proportion to the applied strain and with considerably higher sensitivity (gauge factor = 15) compared to conventional metal foil strain gauges. It is expected that this simple route to fabricate 1D metal nanostructures and semiconductor/metal hybrid nanostructures can be applied to a variety of material combinations, and can be used for numerous applications such as physical sensors (strain, force, flow, etc) and chemical sensors (SPR-based chemical detection, chemiresistor-based biosensors, electrochemical biosensors, etc).

Acknowledgments

This work was supported by Basic Science Research Programs (2008-0062042, 2010-0015290) and Future-based Technology Development Program (Nano Fields) (2009-0082640) through the National Research Foundation (NRF) funded by the Korean government (MEST), and Open Innovation Research Program of Hewlett Packard (HP) Company, USA.

References

[1] Favier F, Walter E C, Zach M P, Benter T and Penner R M 2001 *Science* **293** 2227
[2] Wang C, Daimon H, Lee Y, Kim J and Sun S 2007 *J. Am. Chem. Soc.* **129** 6974
[3] Lee H, Habas S E, Kweskin S, Butcher D, Somorjai G A and Yang P D 2006 *Angew. Chem. Int. Edn* **45** 7824
[4] Roucoux A, Schulz J and Patin H 2002 *Chem. Rev.* **102** 3757
[5] Han Y J, Kim J M and Stucky G D 2000 *Chem. Mater.* **12** 2068
[6] Steinhart M, Jia Z, Schaper A K, Wehrspohn R B, Gösele U and Wendorff J H 2003 *Adv. Mater.* **15** 706
[7] Deng Z and Mao C 2003 *Nano Lett.* **3** 1545
[8] Song Y, Garcia R M, Dorin R M, Wang H, Qiu Y, Coker E N, Steen W A, Miller J E and Shelnutt J A 2007 *Nano Lett.* **7** 3650

[9] Kijima T, Yoshimura T, Uota M, Ikeda T, Fujikawa D, Mouri S and Uoyama S 2004 *Angew. Chem. Int. Edn* **43** 228
[10] Lu X, Chen J, Skrabalak S E and Xia Y 2008 *Proc. IMechE Part N: J. Nanoeng. Nanosyst.* **221** 1
[11] Liang H W, Liu S, Gong J Y, Wang S B, Wang L and Yu S H 2009 *Adv. Mater.* **21** 1850
[12] Hunyadi S E and Murphy C J 2009 *J. Clust. Sci.* **20** 319
[13] Bi Y and Lu G 2008 *Chem. Mater.* **20** 1224
[14] Chen Z, Waje M, Li W and Yan Y 2007 *Angew. Chem. Int. Edn* **46** 4060
[15] Tseng Y K, Huang C J, Cheng H M, Lin I N, Liu K S and Chen I C 2003 *Adv. Funct. Mater.* **13** 811
[16] Bao J M, Zimmler M A, Capasso F, Wang X W and Ren Z F 2006 *Nano Lett.* **6** 1719
[17] Li Q H, Liang Y X, Wan Q and Wang T H 2004 *Appl. Phys. Lett.* **85** 6389
[18] Wang Z L and Song J H 2006 *Science* **312** 242
[19] Johnson J C, Knutsen K P, Yan H Q, Law M, Zhang Y F, Yang P D and Saykally R J 2004 *Nano Lett.* **4** 197
[20] Wu G S, Xie T, Yuan X Y, Li Y, Yang L, Xiao Y H and Zhang L D 2005 *Solid State Commun.* **134** 485
[21] Vayssieres L 2003 *Adv. Mater.* **15** 464
[22] Greene L E, Law M, Goldberger J, Kim F, Johnson J C, Zhang Y, Saykall R J and Yang P D 2003 *Angew. Chem. Int. Edn* **42** 3031
[23] Law M, Greene L E, Johnson J C, Saykally R J and Yang P D 2005 *Nat. Mater.* **4** 455
[24] Greene L E, Yuhas B D, Law M, Zitoun D and Yang P D 2006 *Inorg. Chem.* **45** 7535
[25] Park W I, Yi G C, Kim M Y and Pennycook S J 2002 *Adv. Mater.* **14** 1841
[26] Wu J J and Liu S C 2002 *Adv. Mater.* **14** 215
[27] Yang P D, Yan H Q, Mao S, Russo R, Johnson J C, Saykally R J, Morris N, Pham J, He R R and Choi H J 2002 *Adv. Funct. Mater.* **12** 323
[28] Yao B D, Chan Y F and Wang N 2002 *Appl. Phys. Lett.* **81** 757
[29] Sun Y, Fuge G M and Ashfold M N R 2004 *Chem. Phys. Lett.* **396** 21
[30] Rout C S, Krishna S H, Vivekchand S R C, Govindaraj A and Rao C N R 2006 *Chem. Phys. Lett.* **418** 586
[31] Hsu C L, Lin Y R and Chen I C 2007 *Appl. Phys. Lett.* **91** 053111
[32] Chang S J, Hsueh T J, Chen I C, Hsieh S F, Chang S P, Hsu C L, Lin Y R and Hung B R 2008 *IEEE Trans. Nanotechnol.* **7** 754
[33] Chang S J, Hsueh T J, Chen I C and Huang B R 2008 *Nanotechnology* **19** 175502
[34] Pacholski C, Komowski A and Weller H 2002 *Angew. Chem. Int. Edn* **41** 1188
[35] Jiménez I O, Romero F M, Bastús N G and Puntes V 2010 *Phys. Chem.* C **114** 1800
[36] Willander M, Klason P, Yang L L, Al-Hilli S M, Zhao Q X and Nur O 2008 *Phys. Status Solidi* c **5** 3076
[37] She G W, Zhang X H, Shi W S, Fan X, Chang J C, Lee C S, Lee S T and Liu C H 2008 *Appl. Phys. Lett.* **92** 053111
[38] Müller K H, Herrmann J, Raguse B, Baxter G R and Reda T 2002 *Phys. Rev.* B **66** 075417
[39] Herrmann J, Müller K H, Reda T, Baxter G R, Raguse B, Degroot G J J B, Chai R, Roberts M and Wieczorek L 2007 *Appl. Phys. Lett.* **91** 183105
[40] Vossmeyer T, Stolte C, Ijeh M, Kornowski A and Weller H 2008 *Adv. Funct. Mater.* **18** 1611